

2

AFWAL-TR-84-4184



HOLD-TIME EFFECTS IN ELEVATED  
TEMPERATURE FATIGUE CRACK PROPAGATION

T. Weerasooriya  
T. Nicholas

UNIVERSITY OF DAYTON  
RESEARCH INSTITUTE  
300 COLLEGE PARK DRIVE  
DAYTON, OHIO 45469

MARCH 1985

DTIC  
ELECTE  
MAY 24 1985  
S B D

Interim Report Covering Period January 1983 Through January 1984

APPROVED FOR PUBLIC RELEASE; DISTRIBUTION UNLIMITED

MATERIALS LABORATORY  
AIR FORCE WRIGHT AERONAUTICAL LABORATORIES  
AIR FORCE SYSTEMS COMMAND  
WRIGHT-PATTERSON AIR FORCE BASE, OHIO 45433

AD-A154 146

DTIC FILE COPY

NOTICE

When Government drawings, specifications, or other data are used for any purpose other than in connection with a definitely related Government procurement operation, the United States Government thereby incurs no responsibility nor any obligation whatsoever; and the fact that the government may have formulated, furnished, or in any way supplied the said drawings, specifications, or other data, is not to be regarded by implication or otherwise as in any manner licensing the holder or any other person or corporation, or conveying any rights or permission to manufacture use, or sell any patented invention that may in any way be related thereto.

This report has been reviewed by the Office of Public Affairs (ASD/PA) and is releasable to the National Technical Information Service (NTIS). At NTIS, it will be available to the general public, including foreign nations.

This technical report has been reviewed and is approved for publication.



THEODORE NICHOLAS, Project Engineer  
Metals Behavior Branch  
Metals and Ceramics Division

FOR THE COMMANDER



JOHN P. HENDERSON, Chief  
Metals Behavior Branch  
Metals and Ceramics Division

"If your address has changed, if you wish to be removed from our mailing list, or if the addressee is no longer employed by your organization please notify AFWAL/MLLN, W-PAFB, OH 45433 to help us maintain a current mailing list".

Copies of this report should not be returned unless return is required by security considerations, contractual obligations, or notice on a specific document.

## REPORT DOCUMENTATION PAGE

<b>1a. REPORT SECURITY CLASSIFICATION</b> Unclassified		<b>1b. RESTRICTIVE MARKINGS</b>										
<b>2a. SECURITY CLASSIFICATION AUTHORITY</b>		<b>3. DISTRIBUTION/AVAILABILITY OF REPORT</b> Approved for public release; distribution unlimited										
<b>2b. DECLASSIFICATION/DOWNGRADING SCHEDULE</b>		<b>4. PERFORMING ORGANIZATION REPORT NUMBER(S)</b> AFWAL-TR-84-4184										
<b>6a. NAME OF PERFORMING ORGANIZATION</b> University of Dayton Research Institute		<b>6b. OFFICE SYMBOL</b> <i>(If applicable)</i>	<b>5. MONITORING ORGANIZATION REPORT NUMBER(S)</b> AFWAL-TR-84-4184									
<b>6c. ADDRESS (City, State and ZIP Code)</b> 300 College Park Drive Dayton, Ohio 45469		<b>7a. NAME OF MONITORING ORGANIZATION</b> Materials Laboratory (AFWAL/MLLN) Air Force Wright Aeronautical Laboratories										
<b>8a. NAME OF FUNDING/SPONSORING ORGANIZATION</b>		<b>8b. OFFICE SYMBOL</b> <i>(If applicable)</i>	<b>7b. ADDRESS (City, State and ZIP Code)</b> Wright-Patterson Air Force Base, Ohio 45433									
<b>8c. ADDRESS (City, State and ZIP Code)</b>		<b>9. PROCUREMENT INSTRUMENT IDENTIFICATION NUMBER</b>										
<b>11. TITLE (Include Security Classification/</b> Hold-Time Effects In Elevated Temperature Fatigue Crack Propagation		<b>10. SOURCE OF FUNDING NOS.</b> <table border="1" style="width: 100%; border-collapse: collapse;"> <tr> <th style="width: 25%;">PROGRAM ELEMENT NO.</th> <th style="width: 25%;">PROJECT NO.</th> <th style="width: 25%;">TASK NO.</th> <th style="width: 25%;">WORK UNIT NO.</th> </tr> <tr> <td style="text-align: center;">61102F</td> <td style="text-align: center;">2307</td> <td style="text-align: center;">P1</td> <td></td> </tr> </table>		PROGRAM ELEMENT NO.	PROJECT NO.	TASK NO.	WORK UNIT NO.	61102F	2307	P1		
PROGRAM ELEMENT NO.	PROJECT NO.	TASK NO.	WORK UNIT NO.									
61102F	2307	P1										
<b>12. PERSONAL AUTHOR(S)</b> T. Weerasooriya* and T. Nicholas**												
<b>13a. TYPE OF REPORT</b> Interim	<b>13b. TIME COVERED</b> FROM 1/83 TO 1/84	<b>14. DATE OF REPORT (Yr., Mo., Day)</b> March 1985	<b>15. PAGE COUNT</b> 26									
<b>16. SUPPLEMENTARY NOTATION</b> *UDRI **AFWAL/MLLN												
<b>17. COSATI CODES</b> <table border="1" style="width: 100%; border-collapse: collapse;"> <tr> <th style="width: 33%;">FIELD</th> <th style="width: 33%;">GROUP</th> <th style="width: 33%;">SUB. GR.</th> </tr> <tr> <td> </td> <td> </td> <td> </td> </tr> <tr> <td> </td> <td> </td> <td> </td> </tr> </table>		FIELD	GROUP	SUB. GR.							<b>18. SUBJECT TERMS (Continue on reverse if necessary and identify by block number)</b>	
FIELD	GROUP	SUB. GR.										
<b>19. ABSTRACT (Continue on reverse if necessary and identify by block number)</b> An experimental investigation was conducted to evaluate the effects of hold-times on the fatigue crack growth rate of Inconel 718 at 649°C using compact tension specimens. Tests were run under computer controlled constant K conditions using compliance to determine crack length. Hold-times ranging from 5 to 50 s were applied at maximum, minimum, and intermediate load levels. The data show that hold-times at maximum load were the most damaging in terms of crack growth rate. Hold times greater than 5 s led to purely time-dependent crack growth behavior which was predictable from sustained load data using K as a correlating parameter. Hold-times at minimum or intermediate load levels had little or no effect on crack growth rate. A linear cumulative damage model based solely on fatigue and sustained load data was found to be adequate for spectrum loading as long as the hold-times were at maximum load. <div style="margin-top: 10px;"> <i>Additional keywords: gas turbine aircraft engines</i> </div>												
<b>20. DISTRIBUTION/AVAILABILITY OF ABSTRACT</b> UNCLASSIFIED/UNLIMITED <input type="checkbox"/> SAME AS RPT. <input checked="" type="checkbox"/> DTIC USERS <input type="checkbox"/>		<b>21. ABSTRACT SECURITY CLASSIFICATION</b> Unclassified										
<b>22a. NAME OF RESPONSIBLE INDIVIDUAL</b> Theodore Nicholas		<b>22b. TELEPHONE NUMBER (Include Area Code)</b> (513) 255-2689	<b>22c. OFFICE SYMBOL</b> AFWAL/MLLN									



## TABLE OF CONTENTS

<u>SECTION</u>		<u>PAGE</u>
1	INTRODUCTION	1
2	EXPERIMENTS	3
3	ANALYSIS	6
4	RESULTS AND DISCUSSION	7
5	CONCLUSIONS	24
	REFERENCES	25

## LIST OF ILLUSTRATIONS

<u>FIGURE</u>		<u>PAGE</u>
1	Crack Growth Rate for 1.0 Hz Fatigue Cycle with Hold-Time at Maximum Load. Dished Lines Show Linear Cumulative Damage Model Predictions.	8
2	Crack Growth Rate for N Fatigue Cycles at 1.0 Hz with Hold-Time at Maximum Load.	9
3	Crack Growth per Cycle Block Consisting of N Cycles and a Hold-Time at Maximum Load (Same Data as Figure 2).	11
4	Crack Growth Rate for 1.0 Hz Fatigue Cycle of $R = 0.1$ with Hold-Time at Minimum Load.	13
5	Crack Growth Rate for 1.0 Hz Fatigue Cycle with Hold-Time at Mean Load.	15
6	Crack Growth Rate for 1.0 Hz Fatigue Cycle with Hold-Time at 75 Percent Maximum Load.	18
7	Crack Growth Rate for Modified TF-34 Spectrum.	20
8	Characteristic Time for Constant K and Constant Load Experiments in CT Specimens of Inconel 718 at 649°C.	23

LIST OF TABLES

TABLE

PAGE

1 HEAT TREATMENT FOR ALLOY 718

4

## SECTION 1

### INTRODUCTION

Crack growth calculations for critical structural components in U.S. Air Force gas turbine engines have become an important part of the design and life management procedures in recent years. Accurate crack growth predictions are required as part of a damage tolerant design approach required by the Air Force for all new engines under the recently adopted Engine Structural Integrity Program (ENSIP) specifications. Further, implementation of a retirement-for-cause or on-condition lifing policy for existing engines requires the capability to predict crack growth rates in engine components under actual operating conditions. These conditions include variations in temperature, cyclic frequency, stress ratio, and sustained load hold-time, as well as interactive effects in a typical load spectrum. One of the major problems is to address the effects of hold times at the highest operating temperatures, where turbine disk alloys demonstrate a varying degree of time-dependent material behavior. In particular, the effects of hold-times between single or multiple cyclic loads is not fully understood.

Hold-times in a typical load spectrum for a turbine engine disk represent a condition of constant engine speed and constant temperature. For high-performance military aircraft engines, hold-times ranging from a few seconds to a few minutes are common throughout the load spectrum which is comprised primarily of low frequency fatigue cycles of varying frequencies, amplitudes, and stress ratios. The hold-times can occur at maximum load or at some intermediate load level between the maximum and minimum of the fatigue

loading. These hold-times can contribute to crack growth at high temperatures through a combination of creep and environmental degradation, primarily oxidation, near the crack tip. In nickel-base superalloys, sustained load crack growth is primarily an environmentally enhanced phenomenon with little or no creep present. In the absence of oxygen, the sustained load crack growth rates have been observed to decrease by more than an order of magnitude [1].

Prior work has shown that sustained load crack growth in nickel-base superalloys can be characterized using the linear elastic fracture mechanics (LEFM) stress intensity factor,  $K$ , as the correlating parameter [2,3]. It has also been shown that for very low frequency cycles, fatigue crack growth rates can be reduced from sustained load crack growth data using simple integrations of the fatigue loading cycle [4]. Hold-time effects at maximum load between fatigue cycles were also well predicted from sustained load data. What has not been evaluated, however, is the contribution of sustained loads at stress levels below the peaks of the fatigue cycles and the interactions between cyclic and sustained loads in complex mission spectra. This report presents the results of a systematic investigation to evaluate hold-time effects in elevated temperature fatigue and guidelines for the prediction of engine spectrum crack growth rates at high temperatures.

## SECTION 2

### EXPERIMENTS

A series of tests was performed on compact type specimens of Inconel 718 involving combinations of cyclic loading and hold-times. All test specimens were of identical dimensions having  $H/W = 0.6$ ,  $B = 10$  mm, and  $W = 40$  mm. The Inconel 718 was heat treated to the standard treatment detailed in Table 1. All tests were conducted at a temperature of  $649^{\circ}\text{C}$  in an MTS servohydraulic test machine using a microcomputer in the feedback loop to control the load on the machine. In addition, a microcomputer was used to acquire and process the raw data in real time. All tests were conducted under conditions of constant maximum stress intensity,  $K$ , until steady state crack growth had been achieved. Crack length was determined indirectly from compliance measurements using digital displacement data from an MTS clip gage with quartz extension rods. The specimen was kept in a resistance heated furnace while the air- or water-cooled extensometer was kept outside the furnace through the use of the extension rods. Temperature in the furnace was controlled to less than  $1^{\circ}\text{C}$  and the total temperature gradient on the crack path was kept to less than  $10^{\circ}\text{C}$ .

Digital load-displacement data were fit to a straight line using a least squares minimization procedure incorporated in the microcomputer to determine compliance. Compliance was then converted to crack length using formula detailed in previous works [2,5]. Crack lengths obtained from compliance data were verified by comparing with the optical measurement data obtained from markings on the fracture surfaces. Some of the crack growth rate tests were repeated under identical conditions. The scatter of the growth rate data was found to be less than 10%.

TABLE 1

HEAT TREATMENT FOR ALLOY 718

- STEP 1: Anneal at 968°C (1775°F) for 1 Hour, Then Air Cool to Temperature
- STEP 2: Age Harden at 718°C (1325°F) for 8 Hours, Then Furnace Cool at 56°C/Hr (100°F/Hr) to 621°C (1150°F)
- STEP 3: Age Harden at 621°C (1150°F) for a Total Aging Time in Step 2 and Step 3 of 18 Hours
- STEP 4: Air Cool to Room Temperature

Several types of loading spectrum were used to evaluate the effects of hold-times on the spectrum crack growth rates of Inconel 718 at 649°C. The first test involved a 1 Hz fatigue cycle with a hold-time at maximum load between fatigue cycles of  $R = 0.1$ . The hold times ranged from zero to 500 s and were conducted for values of  $K_{\max}$  of 40 and 27  $\text{MPa}\cdot\text{m}^{1/2}$ . The second series of tests involved the application of a number of fatigue cycles with a hold-time at maximum load interspersed between the blocks of cycles. The number of fatigue cycles ranged from 1 to 50 at  $K_{\max} = 40 \text{ MPa}\cdot\text{m}^{1/2}$  using hold times of either 5 or 50 s. The third type of test involved a single fatigue cycle of 1.0 Hz with  $R = 0.1$  with a hold-time of either 5 or 50 s at a value less than  $K_{\max}$ . In one group of tests, the hold was applied at the minimum load of the  $R = 0.1$  fatigue cycles. Finally, a spectrum consisting of single fatigue cycle of 1 Hz at  $R = 0.1$  followed by 12 cycles of 2 Hz at  $R = 0.5$  and then a hold of 90 s at maximum load was applied. This spectrum was based on a design spectrum on the Air Force TF-34 engine.

### SECTION 3

#### ANALYSIS

A linear cumulative damage model was used to predict crack growth rates for loading spectra consisting of combinations of fatigue cycles and hold-times. The model involved the simple summation of the individual contributions of the cycles and the hold times. The fatigue crack growth rates were obtained from constant K tests at the appropriate frequency and R ratio. The hold-time predictions were obtained from sustained load crack growth tests. Letting  $da/dN$  be the cyclic crack growth rate and  $da/dt$  the sustained load growth rate, the crack growth rate per cycle block consisting of N cycles and a hold time of  $t_H$  is

$$\frac{da}{dN_b} = N \cdot \frac{da}{dN} + t_H \frac{da}{dt} \quad (1)$$

where  $da/dN_b$  is the growth rate per cycle block. There are no interaction effects considered in this simple model.

## SECTION 4

### RESULTS AND DISCUSSION

The first series of tests involved the application of a single fatigue cycle of  $R = 0.1$  at 1 Hz with a hold-time at maximum load between cycles. Two values of maximum  $K$  were used, 40 and  $27.8 \text{ MPa}\cdot\text{m}^{\frac{1}{2}}$  with hold-times ranging from zero (pure fatigue) to 500 s. The data are plotted in Figure 1 as crack growth rate against total cycle time. Note that a total cycle time of 1 s corresponds to no hold-time since the fatigue cycle is at a frequency of 1 Hz. Shown also in Figure 1 (dashed) is the analytical prediction from the linear cumulative damage model. Two things are evident from the results. First, the model predicts the growth rate extremely accurately for the entire range of hold-times. Second, the behavior of this material is very time-dependent. For hold-times in excess of approximately 10 s, the behavior is essentially time-dependent as evidenced by the  $45^\circ$  slope on the log-log plot of growth rate versus cycle time in Figure 1.

The second series of tests involved the application of a block of fatigue cycles with a single hold-time at maximum load interspersed between the cycles. The cycles were again applied at  $R = 0.1$  and 1.0 Hz. The tests were all conducted using a maximum  $K$  of  $40.0 \text{ MPa}\cdot\text{m}^{\frac{1}{2}}$ . The data are plotted as the average growth rate,  $da/dt$ , against the number of fatigue cycles per block,  $N$ , in Figure 2.  $N$  represents the number of fatigue cycles in a block or spectrum which consists of the fatigue cycles and the hold-time. Thus,  $N = 0$  represents the condition of the hold-time without any fatigue cycles. Values of  $N$  ranged from 1 to 100 using hold-times of 5 and 50 s. The solid

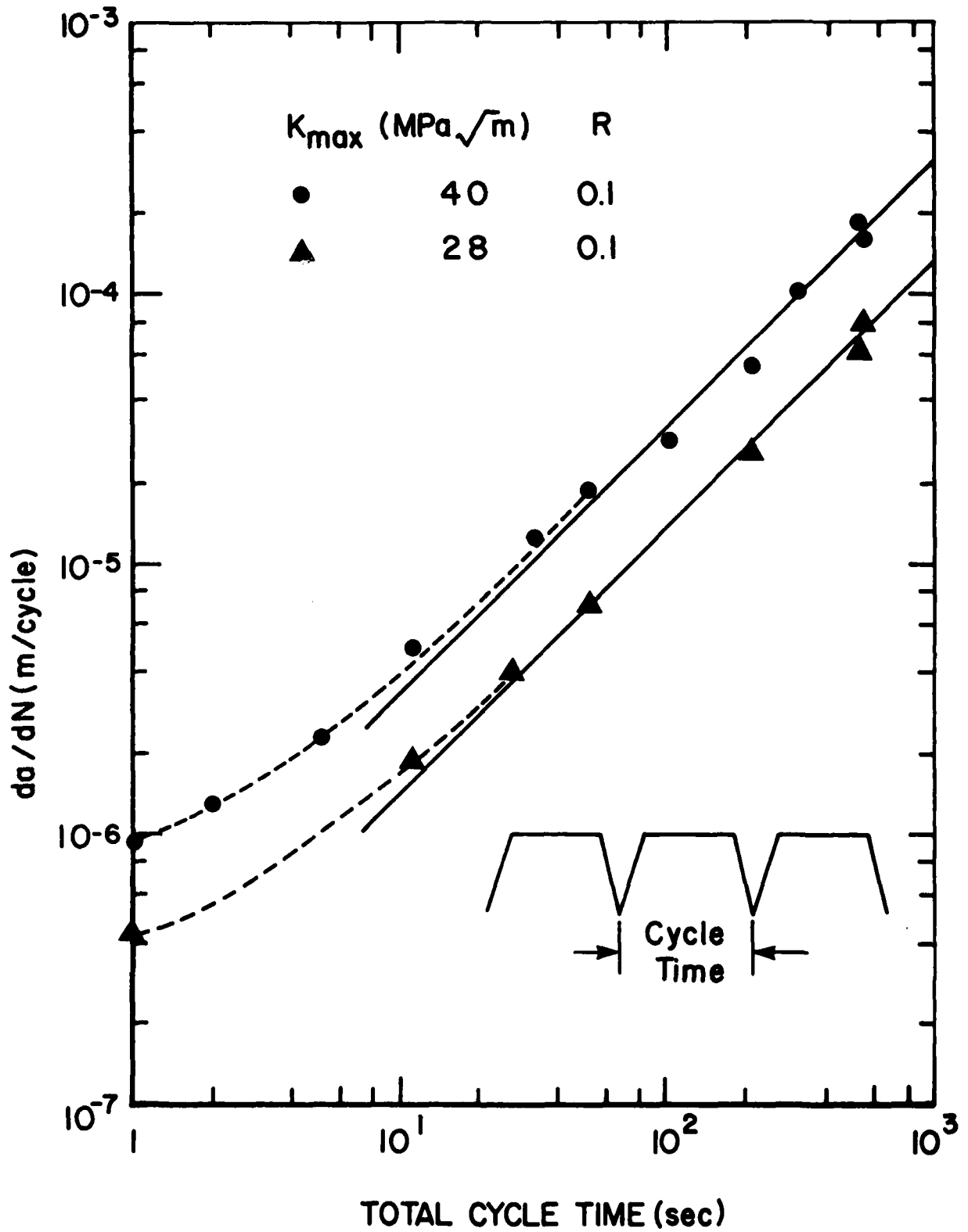


Figure 1. Crack Growth Rate for 1.9 Hz Fatigue Cycle with Hold-Time at Maximum Load. Dashed Lines Show Linear Cumulative Damage Model Predictions.

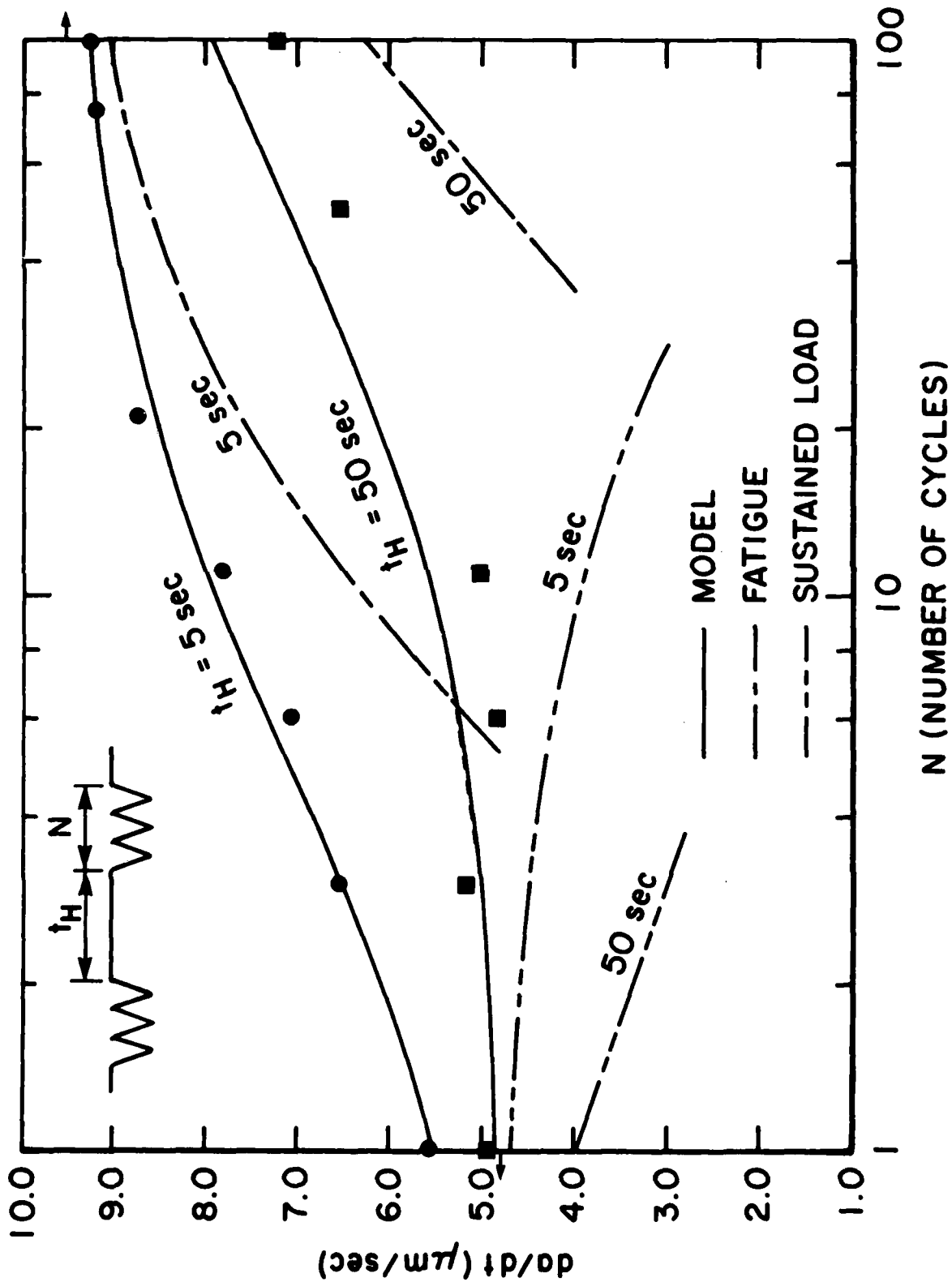


Figure 2. Crack Growth Rate for  $N$  Cycles at 1.0 Hz with Hold-Time at Maximum Load.

lines in Figure 2 represent the predictions of the linear cumulative damage model for the two hold-times. The arrow on the left, representing  $N = 0$ , represents  $da/dt$  for pure sustained load. The arrow on the right represents  $N = \text{infinite}$  which is the growth rate in mm/sec for pure fatigue. The dashed lines represent the analytical predictions considering contributions for only sustained loading or only fatigue loading for the spectrum of  $N$  cycles and a single hold-time at maximum load. It can be readily seen that for anything more than a few cycles up to 100 cycles per block, both sustained load and fatigue contribute to the overall crack growth in this material. Additionally, the linear cumulative damage model works very well in predicting the crack growth rate over the entire range of conditions. For the hold-time of 50 s and larger numbers of cycles, the prediction appears to be slightly high. These data are replotted in Figure 3 using  $N$  as the horizontal axis again. The vertical axis represents the crack extension that occurred during the application of the above block of loading. Three curves in the figure represent three different hold-times; 0, 5, and 50 s. The hold-time of zero represents the case of pure fatigue cycling. The model predictions are the straight lines parallel to the pure fatigue curve. The points along the vertical axis are determined from sustained load crack growth data.

The data points which represent the hold-time of 5 s are parallel to the pure fatigue curve ( $T_H = 0$  s) and shifted by a constant amount which represents the crack growth due to the sustained load of 5 s. In this case, Equation (1) (linear summation model) accurately represents the crack growth per block for constant hold-time. In the case of a hold-time of 50 s, the crack growth per cycle became stabilized to the value of the steady state

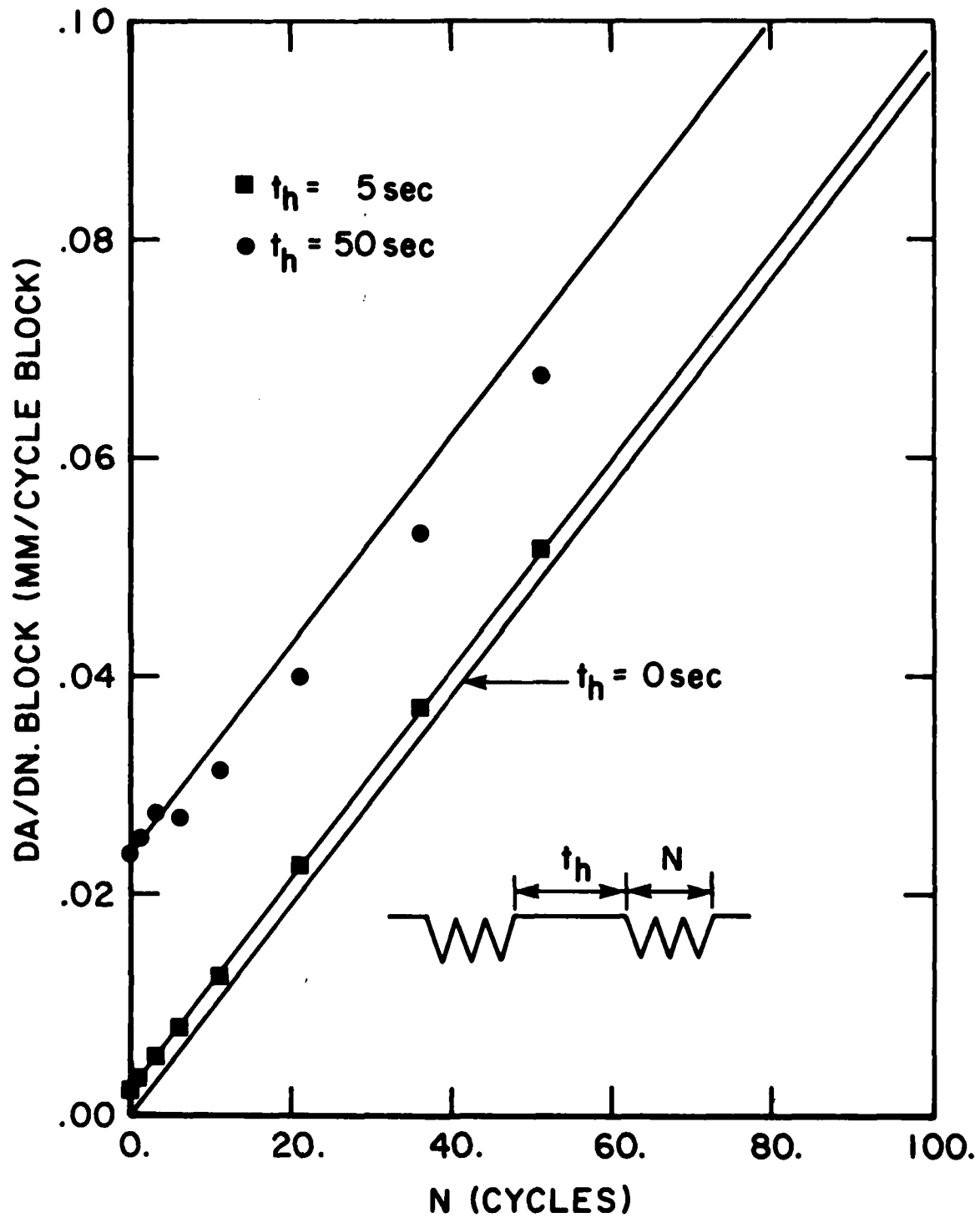


Figure 3. Crack Growth per Cycle Block Consisting of N Cycles and a Hold-Time at Maximum Load (Same Data as Figure 2).

fatigue crack growth rate only after a transition zone ahead of the crack tip was traversed. The size of this long hold-time affected zone is approximately equal to 0.015 mm. Since the growth rate within this zone is smaller than the steady state value of the fatigue crack growth rate, the observed retardation is considered to be due to the blunting of the crack tip. However, for these cases where the maximum stress intensity of both hold-time and cycling are equal, the crack growth retardation which occurs in the very small transition zone is insignificant in the total life prediction. Hence, in the life prediction methodology developed in this paper, the linear summation model given in Equation (1) is adequate and interactions, which are very small, are neglected.

The linear cumulative damage model has also been applied to similar data on IN100 [6]. At 649°C, the behavior is almost exclusively cycle-dependent, but at 732°C, both cycle- and time-dependent behavior were observed as in Inconel 718. In both cases, the model accurately predicts the growth rate for blocks of fatigue cycles with interspersed hold-time at maximum load.

The next series of tests was to evaluate the contribution of a hold-time at minimum load when applied between fatigue cycles of  $R = 0.1$ . In this case, with maximum  $K$  values of 27.8 and 40  $\text{MPa}\cdot\text{m}^{1/2}$ , the sustained load at minimum load ( $K = 4$  and  $K = 2.78 \text{ MPa}\cdot\text{m}^{1/2}$ ) should have no contribution since it is below the threshold values. The data, presented in Figure 4, confirm this supposition. Hold-times at minimum load of up to 500 s did not appear to influence the crack growth rate although there was some variability in the data at the higher maximum  $K$  level of 40  $\text{MPa}\cdot\text{m}^{1/2}$ . It should also be noted

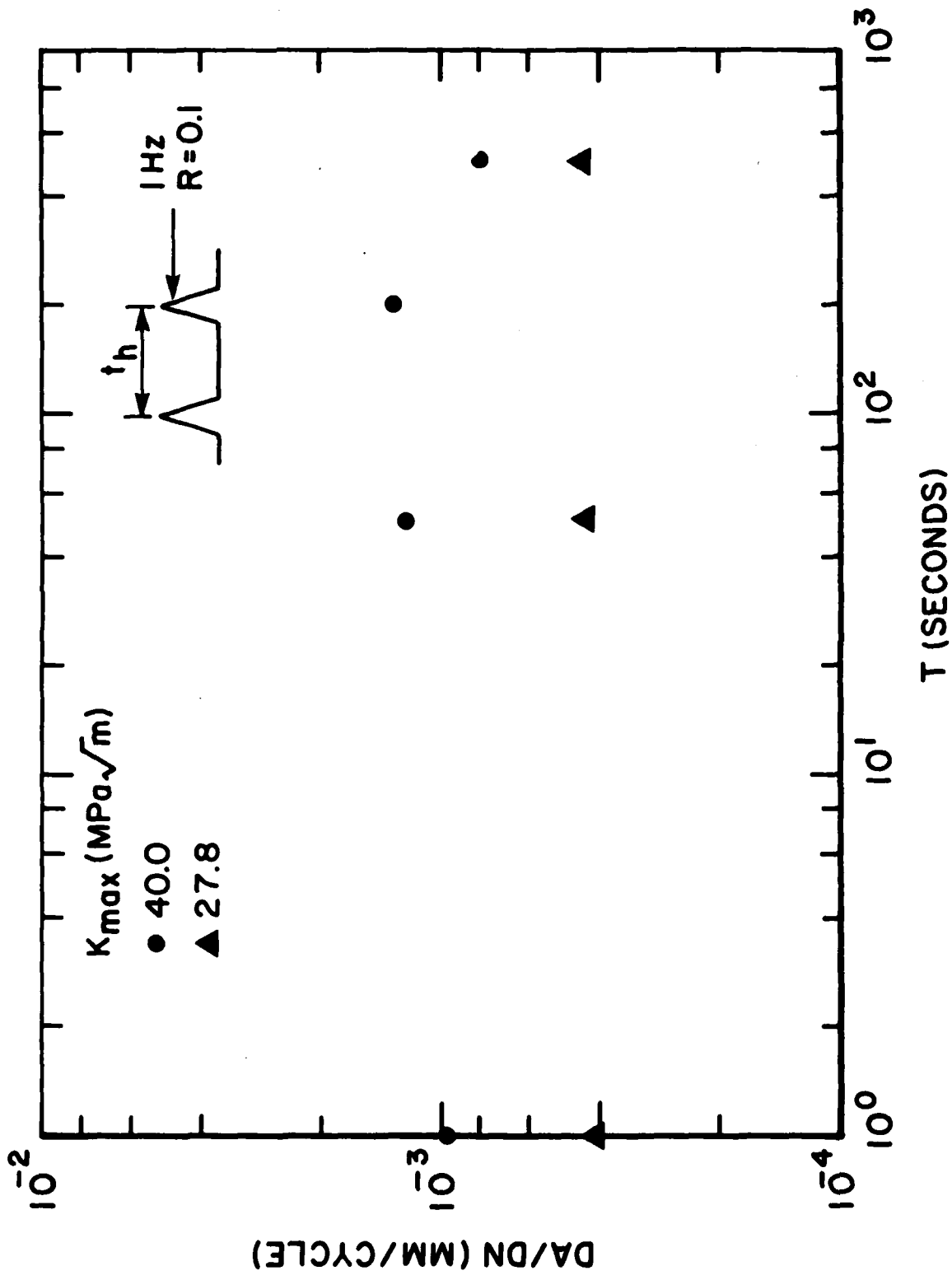


Figure 4. Crack Growth Rate for 1.0 Hz Fatigue Cycle of  $R = 0.1$  with Hold-Time at Minimum Load.

at this point that these data were obtained under conditions of constant  $K$  only after steady state (constant growth rate) conditions were achieved. In many of the tests, initially higher growth rates were observed in changing from other test conditions to conditions with hold times at minimum level. Sadananda and Shahinian [7] observed higher growth rates in constant load range tests using hold-times at minimum load over those observed in pure fatigue tests. They attributed this to an environmentally enhanced degradation of properties even though the hold-time levels were below threshold.

To further evaluate the effects of sustained loads on fatigue crack growth rates, a series of tests were performed using single fatigue cycles with interspersed hold-times at intermediate load levels. The fatigue cycles were applied under constant  $K$  conditions using maximum  $K = 40 \text{ MPa}\cdot\text{m}^{\frac{1}{2}}$ ,  $R = 0.1$ , and a frequency of 1.0 Hz. Sustained load hold-times of 5 and 50 s were applied at 75 percent ( $K = 30 \text{ MPa}\cdot\text{m}^{\frac{1}{2}}$ ) and 55 percent ( $K = 22 \text{ MPa}\cdot\text{m}^{\frac{1}{2}}$ ) of maximum load. In the latter case, the fatigue cycles were applied in two slightly different ways as depicted schematically in Figure 5. The hold-times were applied either after maximum load or after minimum load to evaluate the effect of the sequence of the fatigue loading on the crack growth rates. The main question which we sought to answer was whether the application of the entire range of  $\Delta K$  on loading or unloading made any difference when there was a hold-time between cycles. The results are shown in bar graph format in Figure 5. For hold-times of 5 s, the hold after minimum or maximum load made no difference. The analytical prediction of the growth rate due solely to the fatigue cycle matched the experimental data very closely. If the effect

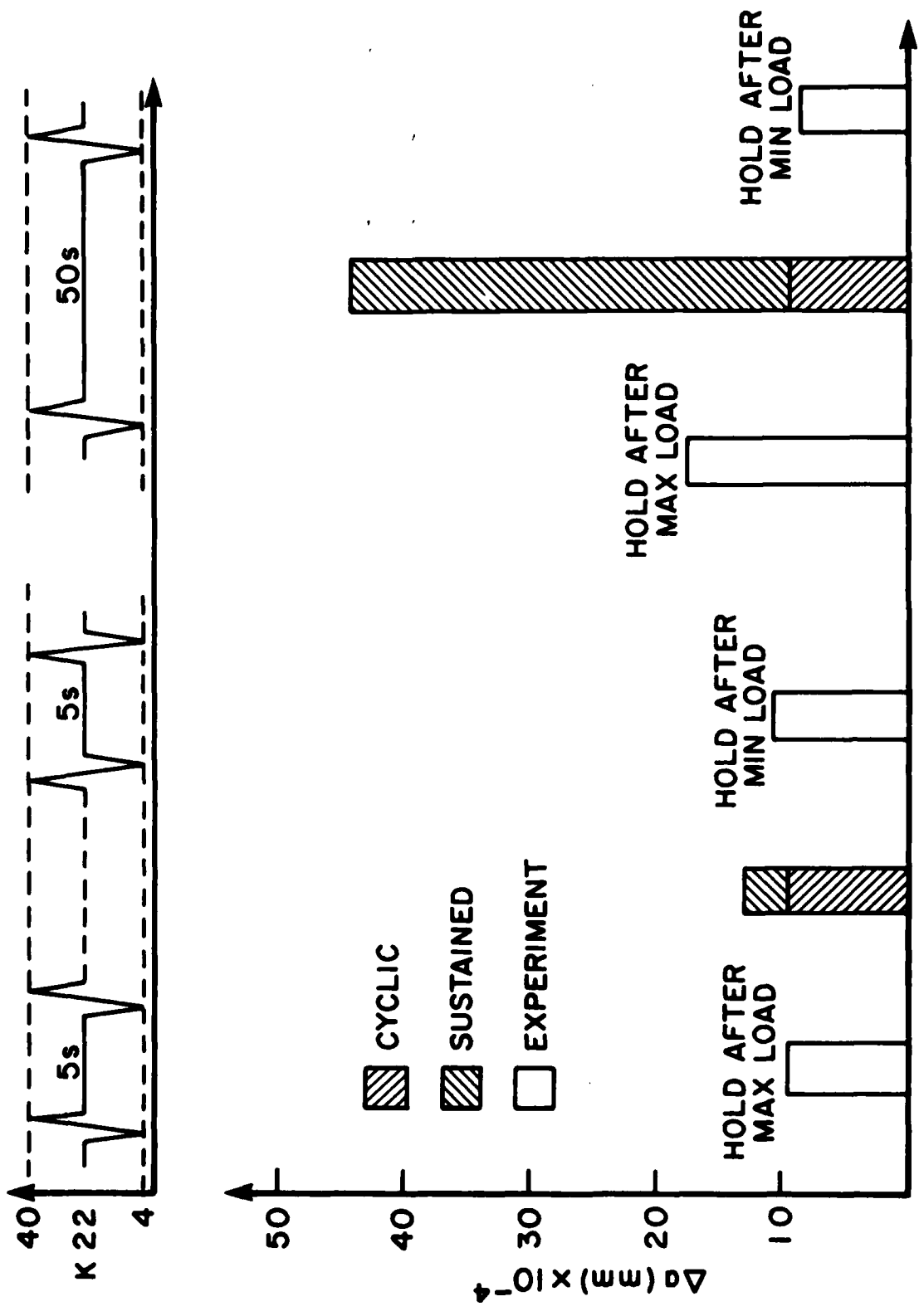


Figure 5. Crack Growth Rate for 1.0 Hz Fatigue Cycle with Hold-Time at Mean Load.

of the hold-time were included in the prediction, the model overpredicts the crack growth rate. In this case, it appears that the hold-time can be neglected in predicting the crack growth rate. When the hold-time was increased by a factor of ten to 50 s, the analytical contribution of the sustained load portion of the load spectrum becomes dominant. The experimental results, however, as seen in Figure 5, show that the growth rate is close to that predicted by the fatigue cycle alone. In the case where the hold-time was applied after maximum load (shown schematically in the figure), the growth rate was higher than when applied after minimum load and certainly higher than that due to fatigue only. There are two possible explanations. The first, and most plausible, is that steady state crack growth had not been achieved under constant K conditions. The total amount of crack extension was approximately 0.3 mm which has been found to be adequate in most cases. We have observed in some data, however, that transient behavior can occur even after crack extensions of this magnitude. This was observed, in particular, in tests with hold-times at minimum load between fatigue cycles. Only continued crack growth under identical conditions, which is very time consuming, could answer these questions. The second possible explanation would be an environmental degradation during the hold-time which would accelerate the growth during the subsequent fatigue cycle where the  $\Delta K$  range is applied during rising or increasing load. This area appears to warrant further study.

For the cases where the sustained load was applied at 75 percent of maximum load, the contribution of the hold-time in the analytical prediction is significant for hold-times of either 5 or 50 s. The experimental

results show, however, that the actual growth rates are very close to those of pure fatigue cycling as shown in Figure 6 (a and b). Note that the analytical contribution of the hold-time, particularly for the 50 s hold-time, is very substantial. In this cases, with sustained loads at 75 percent of maximum load, it appears that the hold-time does not contribute to the overall crack growth.

To further evaluate this hypothesis, the fatigue cycle was changed as shown schematically in Figure 6c. The maximum load of the fatigue cycle, the magnitude of the hold-time, and the amplitude of the sustained load were the same as in the previous case (Figure 6b) but the R-ratio was changed from 0.1 to 0.75. By doing this, the growth rate of the fatigue cycle is significantly reduced because of the smaller range of  $\Delta K$ . The experimental results are compared with the analytical prediction in Figure 6c and show two things. First, the experimental growth rate is significantly less than that predicted due to the sustained load hold-time alone. Second, the experimental growth rate is approximately 2.5 times that predicted due to fatigue cycling alone at  $R = 0.75$ . In the last case, neither fatigue nor sustained load predictions agree with the data while the linear cumulative damage model grossly overpredicts the growth rate. This case can be thought of as a situation where sustained load crack growth is severely retarded by the application of periodic overloads at 50 s intervals. Alternately, it can be viewed as fatigue cycling which is supplemented by a contribution due to sustained load at minimum load. The magnitude of this contribution is certainly non-zero but much less than that which is observed in pure sustained load tests with no fatigue cycles or periodic overloads.

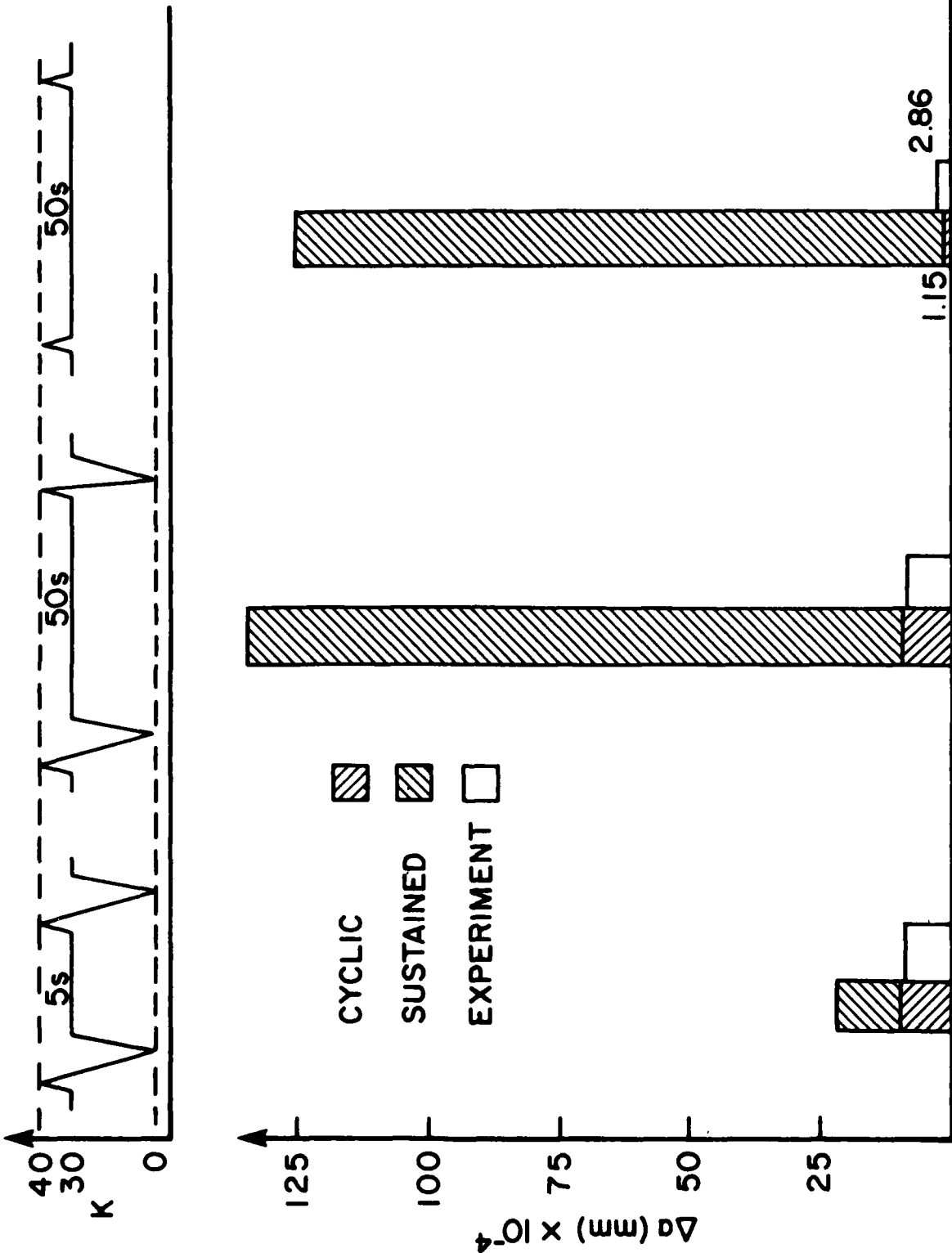


Figure 6. Crack Growth Rate for 1.0 Hz Fatigue Cycle with Hold-Time at 75 Percent Maximum Load.

Finally, to verify the applicability of the simple linear cumulative damage model to engine spectra, an experimental crack growth rate was obtained for the modified TF-34 load spectrum at high temperature. The spectrum is shown in Figure 7, and consists of one cycle of 1 Hz at  $R = 0.1$ , 12 cycles of 2 Hz at  $R = 0.5$ , and a 90 s hold-time at the maximum stress intensity of  $40 \text{ MPa}\cdot\text{m}^{\frac{1}{2}}$ . Experimental growth for one total block of the spectrum and the analytical linear cumulative damage model predictions are given in Figure 7. For this modified spectrum, the analytically predicted cumulative sum of the growth due to three sub blocks of the spectrum is approximately equal to the experimentally predicted crack growth for the total spectrum. Thus, the applicability of the linear cumulative damage model is verified for a typical engine spectrum, where the maximum stress intensity in each sub block of the spectrum is equal. Further studies are required in cases when the maximum stress intensities at each sub spectrum block are not identical.

In all evaluations of crack growth rate behavior, the stress intensity  $K$ , or stress intensity range,  $\Delta K$ , was used for sustained load or cyclic behavior, respectively. For a creeping solid, the energy rate line integral  $C^*$ , derived by Landes and Begley [8], has been found to be more effective in correlating sustained load crack growth rates for some materials. Riedel and Rice [9] have defined a characteristic time  $t_1$  as

$$t_1 = \frac{K_1^2(1 - \nu^2)}{E(n+1)C^*} \quad (2)$$

where  $K$  is the stress intensity,  $\nu$  is Poissons ratio,  $E$  is Young's modulus, and  $C^*$  is the energy rate line integral. If the test time or hold-time is

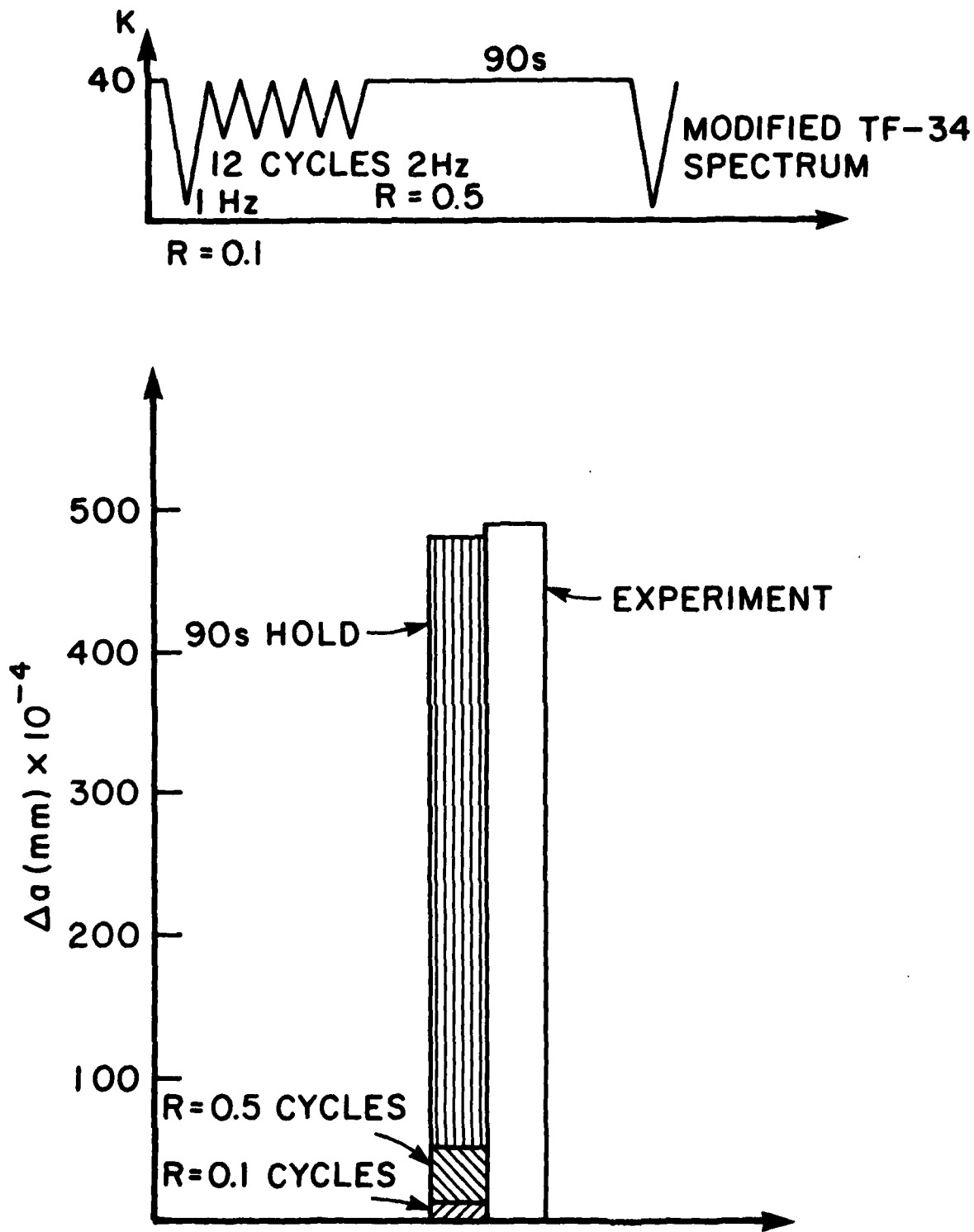


Figure 7. Crack Growth Rate for Modified TF-34 Spectrum.

sufficiently small compared with the characteristic time  $t_1$  in Equation (2), then small scale yielding prevails and  $K$  governs the stress and strain fields ahead of the crack tip. Conversely, for times greater than  $t_1$ ,  $C^*$  is shown to be the correlating parameter for the stress and strain fields and, consequently, crack growth rates. The constant  $n$  is the exponent of the constitutive law for an assumed creeping solid given by

$$\frac{\dot{\epsilon}}{\epsilon_0} = \alpha \left( \frac{\sigma}{\sigma_0} \right)^n \quad (3)$$

where  $\alpha$  is a proportionality constant and  $\epsilon_0$  and  $\sigma_0$  are reference strain rates and stresses, respectively. The line integral  $C^*$  can be determined from simplified methods developed from analogy to elastic-plastic solutions for the J-integral as applied by Saxena [10], for example. In those methods, J-integral solutions, which are based on a constitutive law of the form

$$\frac{\epsilon}{\epsilon_0} = \alpha \left( \frac{\sigma}{\sigma_0} \right)^n \quad (4)$$

are easily converted to  $C^*$  solutions through the replacement of strain and displacements by strain rates and displacement rates, respectively, in the definition of  $J$ . The solutions for  $J$ , in this particular problem of a CT specimen, were taken from results obtained by Kumar, German, and Shih [11] using an estimation scheme and computer program described in detail by Weerasooriya and Gallagher [12]. The value for  $n$  in Equation (3), obtained from a plot of secondary creep rates as a function of stress from an extensive series of tests, was found to be 18.4. The transition times are

plotted in Figure 8 for the cases of tests under constant K and constant P for a CT specimen of Inconel 718 at 649°C. It is clearly seen that the transition times,  $t_1$ , are orders of magnitude larger than the hold-times or test times used in this investigation. It is also noted that for each loading spectrum investigated, constant crack growth rates were obtained when tests were conducted under computer controlled constant K conditions. Thus, K has been established as a valid correlating parameter in this investigation.

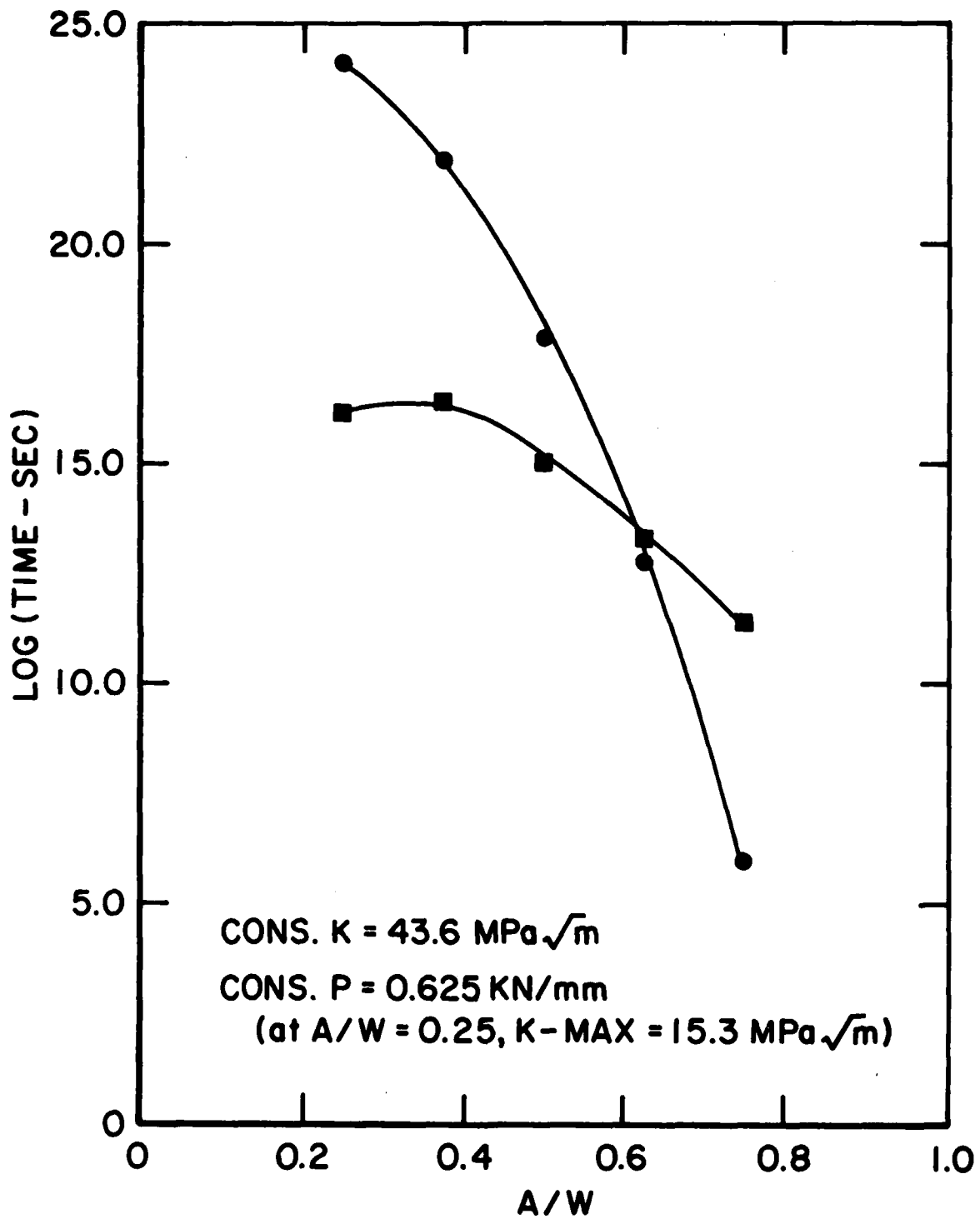


Figure 8. Characteristic Time for Constant K and Constant Load Experiments in CT Specimens of Inconel 718 at 649°C.

## SECTION 5

### CONCLUSIONS

Hold-times at maximum load which occur between single or multiple fatigue cycles contribute to overall crack growth rate in Inconel 718 at 649°C. The magnitude of this contribution is determinable from sustained load crack growth data. A linear cumulative damage model predicts crack growth rates quite accurately over a range of conditions covered in this investigation. Application of hold-times at less than maximum loads between fatigue cycles has less influence than that predicted from sustained load crack growth data. Thus, a linear cumulative damage model overpredicts crack growth rates. In most of the cases investigated, the contribution of the hold-time could be neglected entirely. There was one case, however, where the hold-time could not be neglected but was found to contribute only a small fraction of its effect as determined from sustained load test data. In general, sustained loads appear to be important only when applied at maximum load in a fatigue spectrum. When sustained loads are applied at less than maximum load, their contribution is greatly diminished but they create a situation which involves complex fatigue-sustained load interactions involving possible overload retardation effects.

## LIST OF REFERENCES

1. Stucke, M. et al., "Environmental Aspects in Creep Crack Growth in a Nickel-Base Superalloy," to be published in Proceedings of the Sixth International Conference on Fracture, December 1984.
2. Donath, R. C., Nicholas, T. and Fu, L. S., in Fracture Mechanics: Thirteenth Conference, ASTM STP 743, Richard Roberts, Ed., American Society for Testing and Materials, 1981, pp. 186-206.
3. Ashbaugh, N. E., "Creep Crack Growth Behavior in IN718 in Lab Air," presentation at ASTM 17th National Symposium on Fracture Mechanics, Albany, New York, August 1984.
4. Nicholas, T., Weerasooriya, T., and Ashbaugh, N. E., "A Model for Creep/Fatigue Interactions in Alloy 718," presented at ASTM 16th National Symposium on Fracture Mechanics, Columbus, Ohio, August 1983; to be published in ASTM STP.
5. Saxena, A. and Hudak, S. J., Jr., International Journal of Fracture, Vol. 14, No. 5, October 1978, pp. 453-468.
6. Larsen, J. M. and Nicholas, T., "Cumulative Damage Modeling of Fatigue Crack Growth," presented at AGARD Specialists' Meeting of the Propulsion and Energetics Panel on Engine Cyclic Durability by Analysis and Testing, Lisse, Netherlands, 1984; to be published in AGARD Conference Proceedings.
7. Sadananda, K. and Shahinian, P., Journal of Engineering Materials and Technology, Transactions, American Society of Mechanical Engineers, Vol. 100, 1978, pp. 381-387.
8. Landes, J. D. and Begley, J. A., in Mechanics of Crack Growth, ASTM STP 590, American Society for Testing and Materials, 1976, pp. 128-148.
9. Riedel, H. and Rice, J. R., in Fracture Mechanics (Twelfth Conference), ASTM STP 700, American Society for Testing and Materials, 1980, pp. 112-130.
10. Saxena, A., in Fracture Mechanics (Twelfth Conference), ASTM STP 700, American Society for Testing and Materials, 1980, pp. 131-151.
11. Kumar, V., German, M. D., and Shih, C. F., "Estimation Technique for the Prediction of Elastic-Plastic Fracture of Structural Components of Nuclear Systems," Combined Second and Third Semiannual Report, February 1979 to January 1980 for EPRI, General Electric Company, SRD-80-094.
12. Weerasooriya, T. and Gallagher, J. P., "Determining Crack Tip Field Parameters for Elastic-Plastic Materials via an Estimation Scheme," Technical Report AFWAL-TR-81-4044, Wright-Patterson Air Force Base, Ohio, 1981.